Physics-Based Modeling Aspects of Schottky Diodes for Circuit Design Above 1 THz

José V. Siles*, Jesús Grajal* and Aldo Di Carlo†
(Contact: jovi@gmr.ssr.upm.es)
**Dept. Signals, Systems and Radiocommunications, Technical University of Madrid, Madrid, Spain*
†*Dept. Electronic Engineering, Optolab, University of Rome II Tor Vergata, Rome, Italy*

***Abstract*—This work analyzes some of the physical aspects that must be dealt with for terahertz circuit design based on Schottky diodes beyond 1 THz. The high operation frequencies and the small dimensions that will be required for the devices make it essential to employ physics-based numerical simulators for the device optimization. We present an overview of the possible alternatives and discuss the most adequate ones considering both accuracy and simulation time. As a reference, we employ a Monte Carlo simulator because it provides a numerical solution to the Boltzmann Transport Equation. Since high doping levels will be necessary at these frequencies, the MC analyses should be based on Fermi-Dirac statistics. An efficient method for the inclusion of Fermi-Dirac statistics in MC simulators for non-homogeneous devices is also outlined and the effects of using Fermi-Dirac statistics instead of Maxwell-Boltzmann in Schottky diode models are analyzed.**

I. Introduction

In the recent years, great advances are being made in millimeter-wave solid-state sources resulting in a rapid increase of the available local oscillator (LO) power at frequencies around 100 GHz. Current state-of-the-art LO sources can provide around 400 mW at W-band, and up to several watts can be achieved in the near future [1]. This clearly opens the possibility for the development of LO sources and mixers based on Schottky diodes beyond 2 THz. However, the traditional methods widely employed by designers so far, which are generally based on simple analytical diode models, will not be appropriate for THz circuit design beyond 1-2 THz. At these frequencies, even the validity of those physical models based on simplifications of the Boltzmann Transport Equation (BTE), like Drift-Diffusion (DD) and Hydro-Dynamic models (HD), has to be confirmed.

Therefore, accurate physics-based semiconductor models must be employed for the next generation of both Schottky diode based LO sources and frequency mixers at the THz range. The high operation frequency, the small dimensions that will be required for these devices (with epilayer thicknesses of 100 nm or less) and the high doping concentrations necessary to mitigate carrier velocity saturation will make it crucial to employ very accurate models accounting for the limiting physical mechanisms connected with these device characteristics. However, computational cost must also be accounted for and a trade-off between accuracy and simulation time has to be found.

The goal of this paper is to analyze some of the physical aspects that must be dealt with for terahertz circuit design based on Schottky diodes beyond 1 THz. The main approach consists in using an harmonic balance simulator coupled with a physics-based drift-diffusion model to analyze the device in a self-consistent way together with the embedding circuit [2]. In order to check this approach beyond 1 THz (with short devices and high doping concentrations) we employ a Monte Carlo (MC) simulator as a reference because it provides a numerical solution to the BTE [3]. Moreover, the MC device analysis should be based on Fermi-Dirac statistics in order to account for the semiconductor degeneracy. Fermi-Dirac statistics needs to be implemented by using the energy moment distribution function f(k) at every instant of time instead of the equilibrium Fermi-Dirac distribution function to well control the energy transitions during the MC simulation [4]. Thus, non-equilibrium conditions can be well accounted for during high-frequency RF simulations using MC. An efficient method for the inclusion of Fermi-Dirac statistics in MC simulators for non-homogeneous devices is outlined and the effects of using Fermi-Dirac statistics instead of Maxwell-Boltzmann within the Schottky diode analysis are presented.

It is important to remark that the use of MC device models for terahertz circuit design with harmonic balance methods is prohibitive due to its high computational cost. However, it allows to evaluate and improve other physics-based models that might work reasonably well at THz frequencies with an affordable computational cost.

II. Schottky diode modeling for THz circuit design. Accuracy and Simulation time.

The selection of the most adequate method for semiconductor device simulation depends on two important factors: Accuracy and simulation time. Generally, the more complex the selected model, the higher the computational cost will be. Hence, it is important to choose an adequate approach for the device under study and to appreciate its limits and range of validity. So far the most widely employed method for millimeter-wave and submillimeter-wave Schottky diode based circuit design consist of an harmonic balance (HB) circuit optimization using either simple analytical models available in commercial simulators [5] or more complex physics-based numerical models [2], [6], [7]. In either case, the computational cost of the employed device model acquires a major significance because of the iterative nature of the HB methods, which involves several executions of the nonlinear analysis of the device.

The accuracy in the device simulation is normally determined by how accurately carrier transport is described [3]. Analytical device models based on equivalent circuits (generally included in commercial simulators such as ADS from Agilent) assume that the capacitance and current are function of the present value of the internal voltage. For Schottky diodes, this quasi-static approach has been proved to be valid only up to a few hundred GHz [8] so some empirical adjustments are often necessary for submillimeter-wave circuit design [9]. The advantage of analytical models is their very low computational cost.

The key advantage of physical-based numerical models over analytical ones lies in the fact that they are self-consistent and no empirical adjustment is necessary. Most widely used physical models for semiconductor devices are those based on the Boltzmann Transport Equation, which can be used either directly or through its moments [10]. The BTE formulation (Eq. 1) assumes that the electron dynamics are described by a distribution function $f = f(\vec{r}, \vec{p}, t)$, where $\vec{p}$ is the momentum and $\vec{r}$ is the position of the particle. The term $\partial f/\partial t|_{coll}$ has to do with the variation of the distribution function as a consequence of particle collisions inside the device. Once the distribution function f is known, all the parameters of interest (carrier drift velocities, energy distribution, diffusion coefficients, etc.) can be derived from it. However, finding the exact solution to the Boltzmann's equation is a very difficult task, so approximate approaches are generally employed to simplify the problem [10].

$$\partial f/\partial t + \vec{v} \cdot \nabla_r f + \partial \vec{p}/\partial t \cdot \nabla_p f = \partial f/\partial t|_{coll} \qquad (1)$$

On the one hand, HD numerical models consist of the first three moments of the BTE that give respectively the continuity equations, the current flow equations and the energy balance equations for both electrons and holes. The current flow equations are introduced in the continuity equations resulting in four equations that together with Poisson's equation and the corresponding boundary conditions, define the HD method. Hence, the HD method involves the numerical solving of five coupled nonlinear partial differential equations [3]. On the other hand, DD numerical models consider only the two first moments of the BTE (*electron conservation* and an approximate form of the *momentum conservation*). In this case, only three coupled nonlinear partial differential equations must be numerically solved to simulate the device [11]. However, neglecting *energy conservation* prevents DD models from reproducing nonlocal effects such as the velocity overshoot. This may represent a problem at high frequencies because velocity overshoot might increase the current and modify the high frequency performance of the semiconductor device [3].

In contrast to DD and HD models that are based on simplifications of the BTE, MC simulation provides a numerical solution to the BTE. Thus, all the simplifying approximations can be removed and the real shape of the distribution functions can be computed. In addition, MC simulation accounts for the *scattering* mechanisms occurring inside the device and may include a more detailed physical description of the energy band structure [3], [12].

A rough estimation of the valid operation ranges for the different available physics-based model was given by M. Lundstrom in [3] (see Fig. 1). Nevertheless, the actual validity of a specific model has to be verified for the device and operation conditions under study. Obviously, the best way for this task is by direct comparison between measurements and simulation results [2]. However, MC results are in very close agreement with experimental results [3] and can be employed to validate other device models.

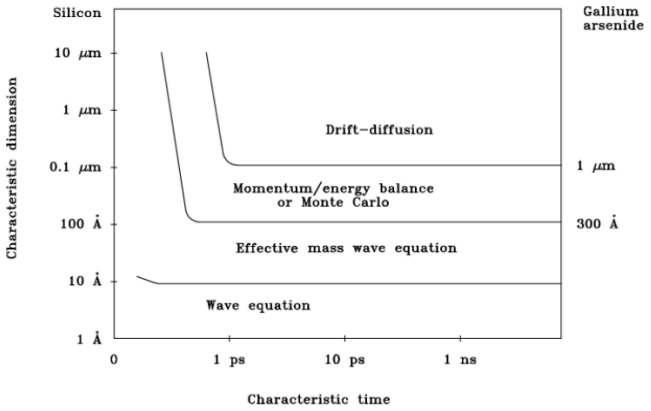

Fig. 1. Estimation of the valid operation range of physics-based semiconductor models by M. Lundstrom [3].

Unfortunately, the excessive simulation time required for MC simulations makes it prohibitive to use MC analysis for the optimization of THz circuits like frequency mixers and multipliers. This is shown in Table I with a comparison between HB simulation times employing both physics-based MC and DD Schottky diode models. Single analysis refers to a Schottky multiplier/mixer simulation for a single operation point whereas circuit optimization involves the joint optimization of all the design parameters (embedding impedances, epilayer thickness and doping, anode area, bias, etc.) in order to maximize the performance at a certain input power and frequency. Note that the computational cost for mixer analysis is much larger than for multipliers. The reason for this is that the time-domain nonlinear response of the diode has to be analyzed along one period of the intermediate frequency resulting in a larger number of voltage samples [13]. Moreover, HB mixer analysis involves a larger number of frequencies, and thereby more HB iterations, because of the necessity to account for both LO and RF harmonics and their intermodulation products [13].

In order to illustrate the usefulness of MC simulators to test other device models, Fig. 2a shows the evolution of the electron velocity as a function of the epilayer thickness for a typical Schottky diode used at millimeter/submillimeter wavelengths. It can be noticed the important increase in the velocity overshoot as the device shrinks from 480 nm to 90 nm according to MC simulations. As already discussed, velocity overshoot is not taken into account in DD models. The difference between MC results (solid curves) and DD results (dashed curves) becomes more evident as the device shrinks. Therefore, DD models seems *a priori* inadequate for terahertz

TABLE I
ANALYSIS AND OPTIMIZATION TIME FOR SCHOTTKY DIODE BASED MIXERS AND MULTIPLIERS USING HARMONIC BALANCE TOGETHER WITH EITHER A MC DEVICE MODEL OR A DD DEVICE MODEL.

	CIRCUIT	Single Analysis	Circuit Optimization (for 1500 analyses)
DD Enhanced DD	MULTIPLIER	0.5 min	~ 12.5 h
	MIXER	40 min	~ 1000 h
MC	MULTIPLIER	140 min	~ 3500 h
	MIXER	3500 min	~ 87500 h

- *Simulation Platform*: Intel P4 3.0 GHz with 4 GB RAM
- Circuit optimization times are indicative (refered to a full optimization involving the analysis of 1500 different operation points)

	Time per Voltage Sample	# Voltage samples (per HB iteration)	# HB iterations (per analyzed operation point)	# Electrons (MC simulation)
MULTIPLIERS	DD → 0.006 s	256	~ 20	~ 50000 *(in this work)*
MIXERS	MC → 1.620 s	~ 5000	~ 80	

circuit design were epilayer thicknesses of the order of 100 nm will be employed. These results are also in agreement with the range of validity predicted in Fig. 1. Moreover, not accounting for velocity overshoot has a notable impact on the simulated Shottky diode I-V curves, which is manifest by the early current saturation in DD results with regard to MC results (Fig. 2b).

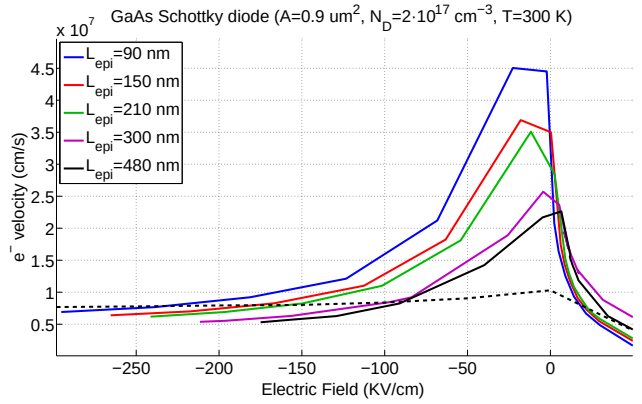

(a)

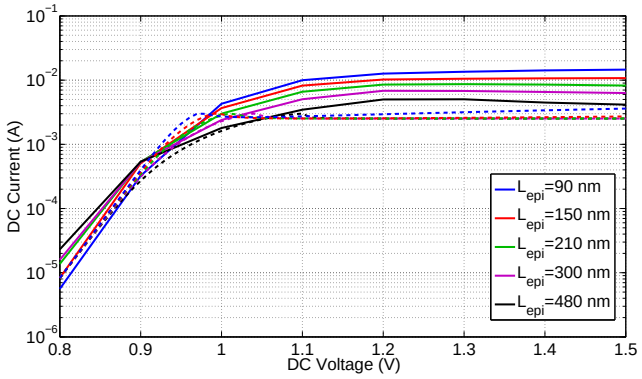

(b)

Fig. 2. MC analysis of the limitations of DD models with device shrinkage: Velocity overshoot (a) and I-V curves (b). MC analysis (solid curves) and DD analysis (dashed curves).

Nevertheless, velocity overshoot occurs at the flatband regime and these operation conditions are not reached in general for Schottky diode based multipliers. On the contrary, minimum conversion losses for Schottky mixers are obtained when flatband voltages are slightly exceeded [14]. Hence, traditional DD simulations are not longer adequate for mixer design due to the limitations shown in Fig. 1. As discussed before, HD models do not experience these limitations but imply the numerical solution of a five-equation system (two more than in DD models), which increases the computational cost. We proposed in [15] an intermediate approach consisting in using MC simulation to redefine the mobility-field characteristics and recombination velocity used in DD Schottky diode models beyond flatband. As illustrated in Fig. 3, our enhanced DD model overcomes the problems shown in Fig. 2 and extends the validity of traditional DD models to submicron devices without adding any extra simulation time.

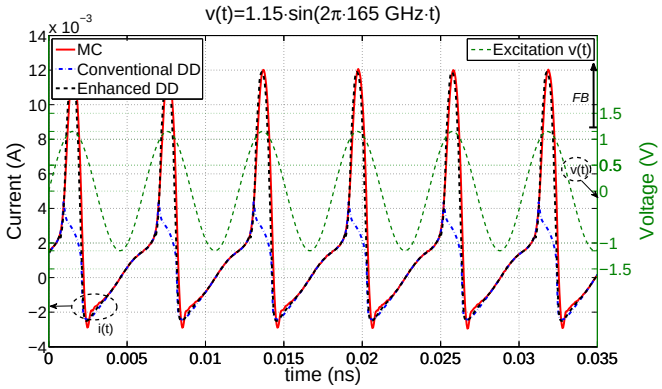

(a)

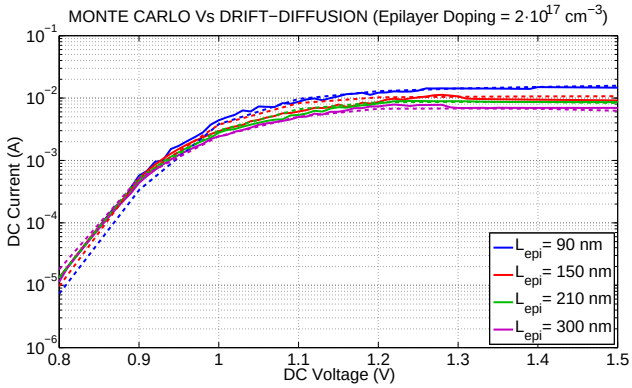

(b)

Fig. 3. MC analysis of the performance of our enhanced DD model presented in [15]: RF current response to a 165 GHz voltage excitation for MC, DD and enhanced DD (a), and I-V curves obtained with MC -solid lines- and DD -dashed lines- (b).

The use of a HB circuit simulator together with our enhanced DD model offers a good trade-off between accuracy and simulation time and might be employed as a first attempt to well optimize Schottky-based circuits beyond 1-2 THz. MC simulations can be used not only to check the validity of the approach but also to analyze other aspects like the evolution of the electron temperature within the device as exemplified in Fig. 4.

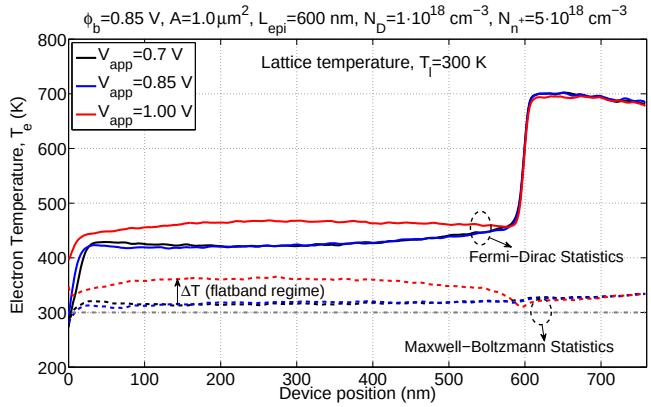

Fig. 4. Electron temperature (T_e) obtained by means of MC simulation (Maxwell-Boltzmann and Fermi-Dirac statistics). Electron temperature is equal to lattice temperature in DD simulations (300 K in this case).

It is important to remark that the electron temperature (T_e) actually represents the average random kinetic energy of the electrons. This corresponds to a temperature only for a non-degenerate Maxwellian distribution function (Maxwell-Boltzmann statistics). For Fermi-Dirac statistics, this quantity accounts for an increase in the electrochemical potential due to degeneracy plus a real-temperature effect [4]. Noise can be as well easily analyzed with MC simulation since it is inherent to MC simulators [16].

III. An Efficient Implementation of Fermi-Dirac Statistics on Schottky diode MC Simulators

MC simulators have a semiclassical nature as they simulate the electron as a classical particle affected by *scattering* mechanisms whose probabilities are obtained according to principles from quantum mechanics. The electrons within the semiconductor behave like *fermions* and consequently the Pauli Exclusion Principle should be included. In this case, the electronic states are described by the Fermi-Dirac statistics instead of by Maxwell-Boltzmann statistics. For MC analysis at terahertz frequencies, where Schottky diodes with highly doped epilayers are necessary, semiconductor degeneracy has to be taken into account. For GaAs, degeneracy occurs for doping levels higher than $4-5\cdot10^{17}\ cm^{-3}$.

The MC code employed herein has been developed at the Tor Vergata University of Rome (Italy). It consists of a band structure with three valleys at the conduction band (the central valley Γ, and the two satellite valleys L and X), and three valence bands (heavy-holes, light-holes and spin-orbit). Spherical constant-energy surfaces are assumed and non-parabolicity correction factors are applied for the calculations [12]. The following scattering events are included: acoustic phonon interaction, polar-optical phonon interaction, electron-plasmon interaction, impurity scattering, electron-hole scattering, intervalley scattering and impact ionization.

The implementation of Fermi-Dirac statistics presented in this section is based on the rejection method proposed by P. Lugli and D.K. Ferry in 1985 for homogeneous devices [4]. MC simulation allows to know the distribution function even in the transient phase. Hence, the actual Fermi-Dirac distribution function $f(\mathbf{k})$, which evolves during the MC simulation (i.e. in RF simulations), can be computed at every instant of time during the MC simulation and employed to control the accepted/rejected energy transitions according to Pauli Exclusion Principle. This technique avoids to use the analytical expression for the equilibrium Fermi-Dirac distribution function (only valid *a priori* in the stationary regime). The method described in this work is an extension of [4] to ensemble MC simulation of heterostructure devices (e.g. Schottky diodes) and performs well even when weighted particles and particle multiplication/cut algorithms are considered within the MC simulation. Note that the use of weighted particles (i.e. one particle represents several electrons) improves MC convergence.

The key point of the algorithm is the adequate normalization of the distribution function $f(\mathbf{k})$ by the maximum number of allowed states (N_c) to properly allow/reject the electron moment transitions after each scattering event [4]. The probability of an electronic transition from state **k** to state **k'** is proportional to the probability that the final state **k'** is unoccupied: $P(\mathbf{k},\mathbf{k'}) \propto f(t,\mathbf{k'})/N_c(t)$. Since $N_c(t)$ depends on the electron concentration n, independent distribution functions are considered for each device layer i (epilayer, n^+-layer and buffer in the case of Schottky diodes):

$$N_c(t,i) = \frac{2\cdot\Omega_c(t,i)\cdot V(t,i)}{8\cdot\pi^3} \tag{2}$$

$\Omega_c(t,i) = \Delta k_x(t,i)\cdot\Delta k_y(t,i)\cdot\Delta k_z(t,i)$ being the unitary k-space volume cell for the MC simulation and $V(t,i) = N_{electrons}(t,i)/n(i)$ being the effective volume in layer i (N_c is derived from the Heisenberg Uncertainty Principle). The index t in the previous equations indicates that these parameters are dynamically recalculated during the MC analysis in order to improve the efficiency of the algorithm. On the one hand, at least 50 particles are always guaranteed for each k-space mesh cell in order to have an accurate enough calculation of the distribution function. Hence, the mesh cell volume $\Omega_c(t,i)$ is dynamically recalculated each time the distribution function is re-evaluated. In addition, maximum and minimum values for the electron moment (k_x,k_y,k_z) are monitored along the analysis in order to well determine the limits for the dynamical definition of the k-space mesh. To avoid unwanted effects when particles with different weights are present in the simulation, especially at the interphases between layers, the effective volume and the number of allowed states are made dependant in the proposed algorithm on the average weight of the electrons within the layer.

On the other hand, the efficiency of the algorithm in terms of simulation time depends on how often the distribution function is recalculated. Fig. 5 shows the performance of the proposed algorithm as a function of the number of MC iterations (N_{FD}) between re-evaluations of the distribution function. It can be seen that good results are obtained for N_{FD} values below 100 MC iterations. Obviously, considering $N_{FD} > 1$ implies that some energy states become slightly overpopulated for small periods of time throughout the analysis. The MC simulation itself rapidly corrects these anomalies so the effect is not noticeable in the overall MC simulation. For $N_{FD} > 200$,

overpopulated energy states are not longer under control and the algorithm fails as can be seen in Fig. 5. Note that a very good accuracy is achieved for $N_{FD} = 50$ with almost no extra time added to the simulation with regard to the use of Maxwell-Boltzmann statistics (see Table II).

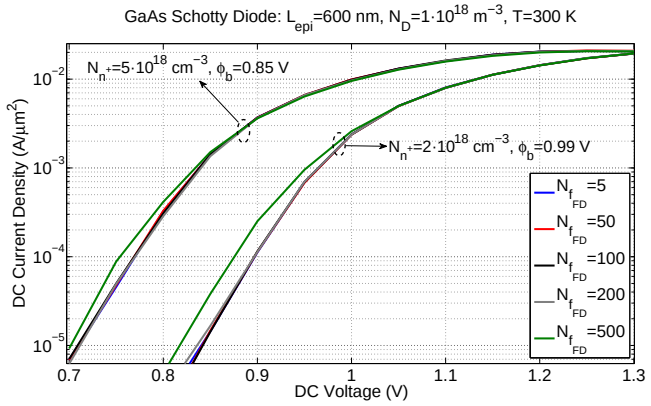

Fig. 5. Fermi-Dirac Monte Carlo I-V Curves as a function of the number of MC iterations N_{FD} between recalculations of the of the distribution function.

TABLE II
FERMI-DIRAC MONTE CARLO SIMULATION TIME AS A FUNCTION OF THE NUMBER OF MC ITERATIONS N_{FD} BETWEEN RECALCULATIONS OF THE OF THE DISTRIBUTION FUNCTION.

	# MC iteration between re-evaluation of Fermi-Dirac distribution function	Time to perform 1000 MC iterations
Monte Carlo (Maxwell-Boltzmann)	----	54 sec
Monte Carlo (Analytical Fermi-Dirac)	----	58 sec
MC (Dynamic Fermi-Dirac) THIS WORK	500	59 sec
	50	62 sec
	5	90 sec
	2	130 sec

To conclude this section, Fig. 6 shows a comparison between the I-V curves obtained with both Maxwell-Boltzmann statistics (blue curves) and Fermi-Dirac statistics (red curves) for two Schottky diodes with epilayer dopings of $1 \cdot 10^{18} cm^{-3}$ and $n^+ - layer$ dopings of $2 \cdot 10^{18} cm^{-3}$ and $5 \cdot 10^{18} cm^{-3}$. From these results, it is evident that Fermi-Dirac statistics must be accounted for in order to well determine the I-V response of highly-doped Schottky diodes. Note that when a low-doped homogeneous diode ($N_D = 1 \cdot 10^{16} cm^{-3}$) is simulated, both Fermi-Dirac and Maxwell-Boltzmann statistics yield the same results since the semiconductor is not degenerated in this case. It can be observed in Fig. 7 that for low dopings similar distribution functions are obtained with both statistics. However, if the doping is increased to $N_D = 1 \cdot 10^{18}$ (degenerate conditions) the MC results obtained with each of the statistics differ significantly. In the case of the Fermi-Dirac statistics, the Pauli exclusion principle forces a large portion of the electrons located in the lower-energy states to move towards higher energy states so the energy distribution function tends to broaden and diminish in comparison to the Maxwell-Boltzmann distribution.

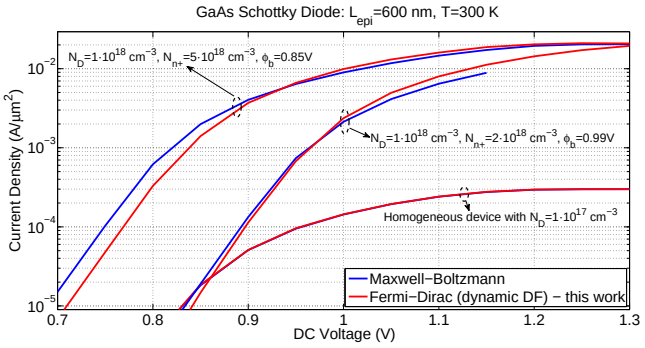

Fig. 6. Performance of the proposed Fermi-Dirac implementation: Monte Carlo simulated I-V curves.

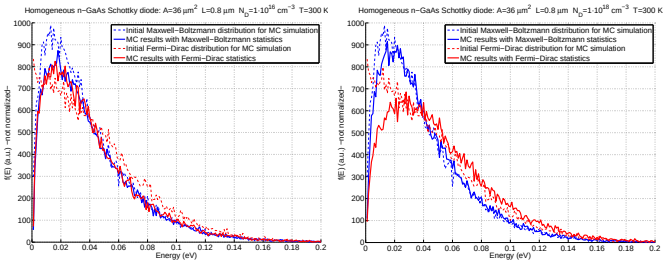

(a) $N_D = 1 \cdot 10^{16}\ cm^{-3}$ (b) $N_D = 1 \cdot 10^{18}\ cm^{-3}$

Fig. 7. Resultant energy distribution functions for a low-doped layer (non-degeneracy case) -left- and a highly-doped layer (degeneracy case) -right-. MC results with Maxwell-Boltzmann statistics (blue curves) and Fermi-Dirac statistics (red curves). Dashed lines represent the initial distribution functions employed for the MC simulations.

IV. PHYSICAL SCHOTTKY-BASED CIRCUIT DESIGN BEYOND 1 THZ

To exemplify those aspects that have been dealt with in the previous sections, we present here a brief study on the theoretically achievable performance of Schottky based frequency doublers at 2.4 THz and 4.8 THz. The analysis are performed by means of the HB circuit simulator coupled with the physics-based enhanced DD model described in [2], [15]. In order to investigate the adequacy of this approach beyond 1 THz we have firstly compared the predicted Schottky diode responses obtained with both the MC and the DD Schottky diode model. A sinusoidal voltage excitation, $V = -2 + 2.85 \cdot sin(\omega_0 t)$, has been considered since it provides a good representative case where the diodes are driven covering almost the whole range between breakdown and forward conduction. It can be noticed in Fig. 8 that the results are quite similar with both simulators. For example, peak to peak amplitudes and waveform slopes are identical. A certain difference can be appreciated at the maximum current peaks. Nevertheless, the general good agreement leads us to think that the considered method may represent a good approach to well estimate the achievable multiplier performances at these frequency ranges. Note that both Maxwell-Boltzmann and Fermi-Dirac statistics provides similar results for these specific devices.

It is well known that for multiplier design above 1-2 THz, where the available input power is very low to provide a sufficient voltage swing of the nonlinear C-V curve, best per-

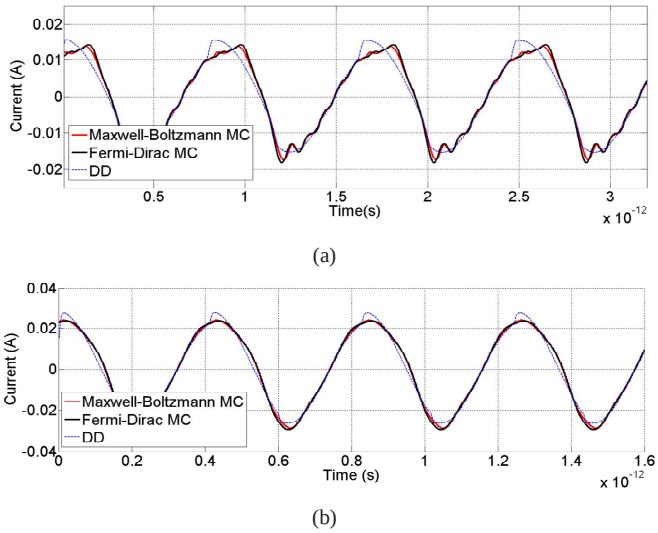

Fig. 8. MC and DD Schottky diode model response to a voltage excitation of 1.2 THz(a) and 2.4 THz (b): $V = -2 + 2.85 \cdot sin(\omega_0 t)$ Volts (T=300 K). GaAs Schottky diodes feature: $A = 0.5\mu m^2$, $L_{epi} = 100nm$, $N_D = 1 \cdot 10^{18} cm^{-3}$, $N_{n+} = 5 \cdot 10^{18} cm^{-3}$).

formance will be obtained for biasless or slightly forward bias designs because of the higher nonlinearity of the capacitance under these circumstances. High doping concentrations ($5{\cdot}10^{17}$ cm^{-3} or higher) need to be considered to mitigate the effect of carrier velocity saturation leading to very short space charge regions. Hence, epilayer thicknesses must be as shorter as possible to reduce the contribution of the non-depleted region of the epilayer to the overall series resistance [2].

Simulation results for a 2.4 THz Schottky diode doubler and a 4.8 THz doubler are respectively shown in Figs. 9 and 10. We have considered and epilayer thickness of 100 nm for the 2.4 THz doubler and a 75 nm epilayer for the 4.8 THz doubler. Epilayer doping concentrations from $5 \cdot 10^{17}$ cm^{-3} to $1 \cdot 10^{18}$ cm^{-3} are analyzed. The n^+-layer doping is $5 \cdot 10^{18}$ cm^{-3} in all the cases. Two important conclusions can be derived from these results. On the one hand, worse results are obtained when using a $1{\cdot}10^{18}$ cm^{-3} doping level due to the reduction of the space charge region that causes an increase in the series resistance. On the other hand, a very precise definition of the optimum values for the design parameters is mandatory, especially for the 4.8 THz doubler.

For the 2.4 THz doubler, a maximum efficiency of 4 % could be theoretically achieved for a 0.5 μm^2 anode area assuming a 1 mW input power per anode ($R_s = 35\Omega, C_{j0} = 1.16fF$). For the 4.8 THz doubler much lower anode areas are necessary due to the lower available input power (40 μW per anode assumed in this work). We have assumed a minimum limit for the anode area of 0.2 μm^2 ($R_s = 80\Omega, C_{j0} = 0.47fF$) and tried to compensate the high required input power by varying the DC bias voltage (towards forward conduction). Note that the peak efficiency is obtained at a lower input power as bias voltage is increased. For 0.8 V, the efficiency drops due to the change between varactor and varistor modes of operation as shown in Fig. 10. This transition coincides with an increase in both the real part and the imaginary part of the optimum resistance at the fundamental frequency (shown impedances are matched for each analyzed input power). This factor is also responsible of the fast degradation of the doubler efficiency beyond a certain input power level.

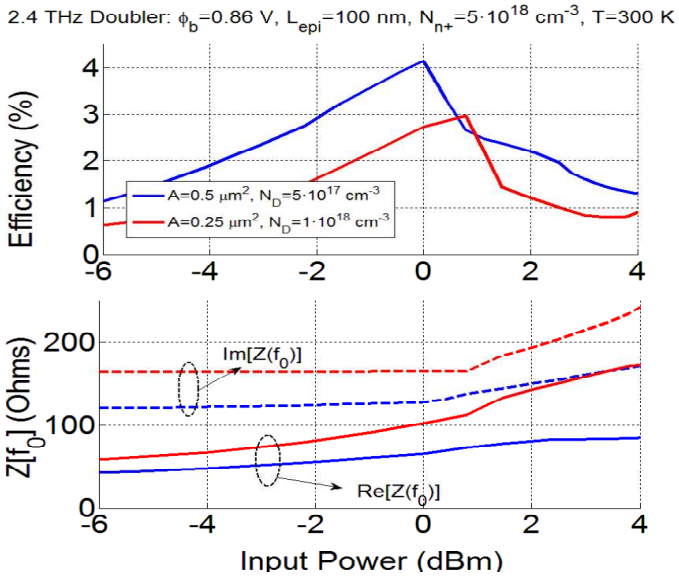

Fig. 9. Theoretically achievable performance for Schottky doublers at 2.4 THz for a 2 mW input power at 1.2 THz (1 mw per anode) and 300 K. Impedances are referred to a single anode (impedances seen from device terminals).

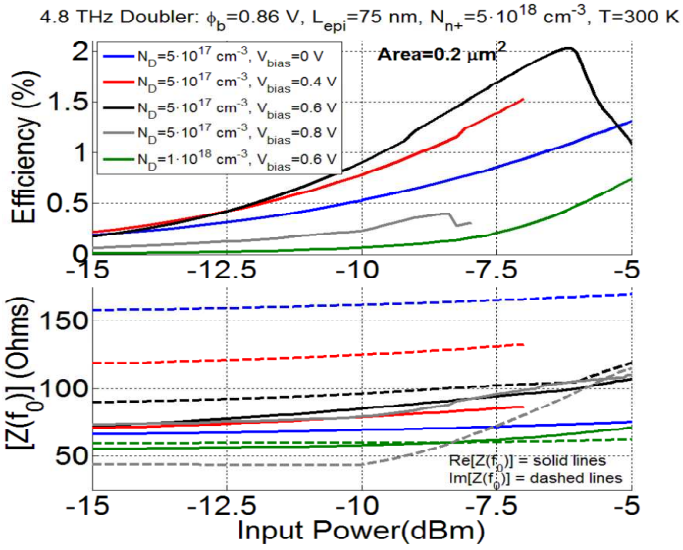

Fig. 10. Theoretically achievable performance for Schottky doublers at 4.8 THz for a 80 μW (-11 dBm) input power at 2.4 THz (40 μW per anode) and 300 K. Impedances are referred to a single anode (impedances seen from device terminals).

To summarize, the low available input power and the circuit sensitivity makes it essential to utilize very accurate device models able to well determine the correct device impedances and properly optimize the circuits. Due to the high sensitivity of the circuit optimization, tuning elements like using DC bias to compensate possible circuit imbalance will not be effective

if the employed model for the circuit design does not guarantee a sufficient accuracy.

Once the device has been optimized by means of HB simulation, MC codes can be employed to evaluate additional aspects like the evolution of the electron temperature within the device. To exemplify this, Fig. 11 shows that the electron temperature remains almost constant (and equal to the lattice temperature: $T_e = T_l = 300K$) along the RF current cycle. However, electron temperature within the active layer vary between 400K and 700K for the 2.4 THz case, and from 350K to 400K for the 4.8 THz due to the lower input power. For these analyses, the MC simulator has been driven with the actual voltage RF waveforms at the Schottky diode terminals resulting from the HB simulation (assuming 1 mW/anode at 2.4 THz and 40 μW/anode at 4.8 THz).

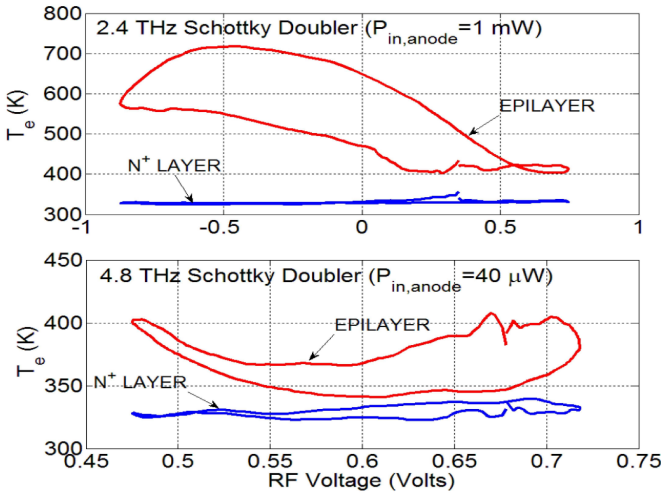

Fig. 11. MC simulation of the RF electron temperature for the analyzed 2.4 THz and 4.8 THz doublers over the RF voltage swing.

V. Conclusion

The use of harmonic balance simulators together with accurate physics-based device models represents the most appropriate way for terahertz circuit design since both the external circuit and the device structure can be simultaneously optimized in a self-consistent way. In this work we have briefly discussed several available device models and its suitability for Schottky based circuit design and optimization beyond 1 THz in terms of accuracy and computational cost. Our harmonic balance simulator featuring an enhanced DD model with improved definition of the mobility-field characteristics offers a good trade-off between simulation time and accuracy. According to HB simulation results, a theoretically achievable performance of $\sim 4\ \%$ might be achieved for 2.4 THz doublers, and $\sim 2\ \%$ for 4.8 THz doublers. MC simulation results have been used to give confidence to the results obtained with this approach. Moreover, an efficient implementation of Fermi-Dirac statistics in the MC simulator has been presented and the impact of using Fermi-Dirac statistics instead of Maxwell-Boltzmann statistics in the simulation of highly-doped n-GaAs Schottky diodes has been discussed.

Acknowledgment

This work was supported by the Spanish National Research and Development Program under projects TEC2008-02148 and TeraSense (Consolider-Ingenio 2010, CSD2008-00068).

References

[1] J. S. Ward, G. Chattopadhyay, J. Gill, H. Javadi, C. Lee, R. Lin, A. Maestrini, F. Maiwald, I. Mehdi, E. Schlecht, and P. Siegel, "Tunable broadband frequency-multiplied terahertz sources," *33rd International Conference on Infrared, Millimeter and Terahertz Waves*, September 2008.

[2] J. V. Siles and J. Grajal, "Physics-based design and optimization of Schottky diode frequency multipliers for THz applications," *Accepted for IEEE Transactions on Microwave Theory and Techniques, Special Issue on "THz Technology: Bridging the Microwave-to-Photonics Gap"*, 2010.

[3] M. S. Lundstrom, *Fundamentals of carrier transport*. Addison-Wesley, 1990.

[4] P. Lugli and D. K. Ferry, "Degeneracy in the ensemble Monte Carlo method for high-field transport in semiconductors," *IEEE Transactions on Electron Devices*, vol. ED-32, no. 11, pp. 2431–2437, November 1985.

[5] A. Maestrini, J. S. Ward, J. J. Gill, H. S. Javadi, E. Schlecht, C. Tripon-Canseliet, G. Chattopadhyay, and I. Mehdi, "A 540-640 GHz high-efficiency four-anode frequency tripler," *IEEE Transactions on Microwave Theory and Techniques*, vol. 53, no. 9, pp. 2835–2843, September 2005.

[6] R. E. Lipsey, S. H. Jones, J. R. Jones, T. W. Crowe, L. F. Horvath, U. V. Bhapkar, and R. J. Mattauch, "Monte Carlo harmonic-balance and drift-difussion harmonic-balance analyses of 100-600 GHz Schottky barrier varactor frequency multipliers," *IEEE Transactions on Electron Devices*, vol. 44, no. 11, pp. 1843–1850, November 1997.

[7] J. Grajal, V. Krozer, E. Gonzalez, F. Maldonado, and J. Gismero, "Modelling and design aspects of millimeter-wave and submillimeter-wave Schottky diode varactor frequency multipliers," *IEEE Transactions on Microwave Theory and Techniques*, vol. 48, no. 4, pp. 700–711, April 2000.

[8] S. A. Maas, *Non-linear Microwave Circuits*. Artech-House, Inc. Boston-London, 1993.

[9] N. Erickson, "Diode frequency multipliers for terahertz local-oscillator applications," *In. Proc. SPIE Advanced Technology MMW, Radio and Terahertz Telescopes*, pp. 75–84, March 1998.

[10] S. Selberherr, *Analysis and Simulation of Semiconductor Devices*. Springer-Verlag. Wien-New York, 1984.

[11] P. J. C. Rodrigues, *Computer-aided analysis of nonlinear microwave circuits*. Artech-House, Inc. Boston-London, 1997.

[12] C. Jacoboni and P. Lugli, *The Monte Carlo method for semiconductor device*. Springer-Verlag Wien New York, 1989.

[13] J. V. Siles, J. Grajal, V. Krozer, and B. Leone, "A CAD tool for the design and optimization of Schottky diodes mixers up to THz frequencies," *In Proc. of the 16th International Symposium on Space Terahertz Technology*, pp. 477–482, May 2005.

[14] T. W. Crowe, W. L. Bishop, D. W. Porterfield, J. L. Hesler, and R. M. Weikle II, "Opening the Terahertz window with integrated diode circuits," *IEEE Journal of Solid-State Circuits*, vol. 40, no. 10, pp. 2104–2110, October 2005.

[15] J. V. Siles and J. Grajal, "Design of submillimeter schottky mixers under flat-band conditions using an improved drift-diffusion model," *IEEE Microwave and Wireless Component Letters*, vol. 19, no. 3, pp. 167–169, March 2009.

[16] J. G. Adams, T. W. Tang, and L. E. Kay, "Monte carlo simulation of noise in GaAs semiconductor devices," *IEEE Transactions on Electron Devices*, vol. 41, no. 4, pp. 575–581, April 1994.